

# A systematic profile of clinical inhibitors responsive to EGFR somatic amino acid mutations in lung cancer: implication for the molecular mechanism of drug resistance and sensitivity

Xinghao Ai · Yingjia Sun · Haidong Wang ·  
Shun Lu

Received: 2 September 2013 / Accepted: 25 February 2014 / Published online: 22 March 2014  
© Springer-Verlag Wien 2014

**Abstract** Human epidermal growth factor receptor (EGFR) has become a well-established target for the treatment of patients with non-small cell lung cancer (NSCLC). However, a large number of somatic mutations in such protein have been observed to cause drug resistance or sensitivity during pathological progression, limiting the application of reversible EGFR tyrosine kinase inhibitor therapy in NSCLC. In the current work, we describe an integration of in silico analysis and in vitro assay to profile six representative EGFR inhibitors against a panel of 71 observed somatic mutations in EGFR tyrosine kinase domain. In the procedure, the changes in interaction free energy of inhibitors with EGFR upon various mutations were calculated one by one using a rigorous computational scheme, which was pre-optimized based on a set of structure-solved, affinity-known samples to improve its performance in characterizing the EGFR-inhibitor system. This method was later demonstrated to be effective in inferring drug response to the classical L858R and G719S mutations that confer constitutive activation for the EGFR kinase. It is found that the

Staurosporine, a natural product isolated from the bacterium *Streptomyces staurosporeus*, exhibits selective inhibitory activity on the T790M and T790M/L858R mutants. This finding was subsequently solidified by in vitro kinase assay experiment; the inhibitory IC<sub>50</sub> values of Staurosporine against wild-type, T790M and T790M/L858R mutant EGFR were measured to be 937, 12 and 3 nM, respectively.

**Keywords** Epidermal growth factor receptor · Somatic amino acid mutation · Drug resistance and sensitivity · Kinase inhibitor · Non-small cell lung cancer

## Introduction

Receptor tyrosine kinase (RTK) superfamily represents a subgroup of transmembrane proteins with an intrinsic tyrosine kinase activity which determines various cellular functions as diverse as growth, differentiation and cell motility or survival (Prenzel et al. 2001). The member of RTK, human epidermal growth factor receptor (EGFR), has received particular attention in recent years owing to their strong association with malignant proliferation. The EGFR is a key cell-surface receptor which plays a crucial role in signal transduction pathways that regulate important cellular behaviors such as differentiation and proliferation. Increased levels of EGFR gene expression are observed in various cancers including head and neck, breast, colorectal, lung, prostate, kidney, ovary, brain, pancreas and bladder carcinomas. In particular, extending previous observations of almost two decades ago (Veale et al. 1987), recent retrospective analyses have reported EGFR overexpression in 62 % of non-small cell lung cancer (NSCLC) cases, and its expression is correlated with a poor prognosis (Sharma et al. 2007).

---

X. Ai and Y. Sun contributed equally to this work.

---

**Electronic supplementary material** The online version of this article (doi:10.1007/s00726-014-1716-0) contains supplementary material, which is available to authorized users.

---

X. Ai · Y. Sun · S. Lu (✉)  
Lung Tumor Clinical Medical Center, Shanghai Chest Hospital,  
Shanghai Jiao Tong University, Shanghai 200030, China  
e-mail: shun\_lu@126.com

H. Wang  
Department of Oncology, Third Military Medical University,  
Chongqing 400038, China

Given its central role in regulating cell proliferation, survival and migration in normal and cancerous cells, much effort has been devoted to development of cancer therapeutics targeting EGFR. Up to date, three EGFR tyrosine kinase inhibitors (TKIs), i.e. Erlotinib, Gefitinib and Lapatinib, have been approved by FDA for cancer therapy and also a number of second- and third-generation TKIs such as afatinib, neratinib and WZ4002 are in clinical or preclinical development (Ohashi et al. 2013). However, EGFR TKI treatment is not curative in patients because of both primary and secondary treatment resistance (Lin and Bivona 2012). One of important factors to cause drug resistance is the somatic mutations in EGFR tyrosine kinase (TK) domain, which were observed to elicit constitutive activation of the kinase by destabilizing the auto-inhibited conformation that is normally maintained in the absence of ligand stimulation (Shigematsu and Gazdar 2006). The somatic mutations may alter TKI sensitivity to EGFR by several mechanisms. For example, it was reported that the marketed inhibitor Gefitinib binds 20-fold more tightly to EGFR L858R mutant than to the wild-type enzyme, whereas the G719S mutation would considerably reduce the Gefitinib affinity to EGFR (Yoshikawa et al. 2013). In addition, the T790M mutation in EGFR was thought to cause drug resistance by increasing the kinase affinity for ATP rather than by sterically blocking the binding of TKIs (Yun et al. 2008).

The complexity of the molecular mechanism underlying drug response and susceptibility to EGFR mutations promotes us to systematically investigate the complete interaction profile of EGFR mutants with diverse inhibitors. However, it is too time-consuming and expensive to experimentally test the affinities of all existing TKIs to hundreds of potential residue mutations in EGFR TK domain. Alternatively, in silico approach provides a promising way to virtually characterize protein–chemical interactome in a high throughput manner. In the current study, an integrative strategy of rigorous quantum mechanics/molecular mechanics (QM/MM) analysis and empirical solvent model was described to fast and reliably characterize the binding free energy change of small-molecule inhibitors upon EGFR mutations based on their complex three-dimensional structure. With this method, we were able to profile 6 EGFR inhibitors, including 3 FDA-approved drugs, 2 compounds that are currently under clinical development and a natural kinase blocker, as well as its natural substrate ATP against a panel of 71 observed somatic mutations in EGFR TK domain. On this basis, we examined the specificity and sensitivity of different compound entities binding to a wide spectrum of EGFR mutants, and investigated the molecular mechanism and biological implication underlying drug response

to EGFR mutations. We also identified several potential mutations that might cause drug resistance by directly influencing the non-bonded interaction of EGFR with inhibitors or by indirectly addressing allosteric effect on the kinase structure, which were verified by a following in vitro kinase assay experiment. This study would help to establish a systematic kinase–small-molecule interaction profile for clinical compounds across various EGFR mutants.

## Materials and methods

### Data preparation

#### *Structure-based data set of wild-type and mutant EGFR–inhibitor affinities*

We have compiled 20 affinity data associated with binding of the three FDA-approved EGFR inhibitors, i.e. Gefitinib, Erlotinib and Lapatinib, to wild-type and mutant EGFR from the publications contributed by Zarrinkar and co-workers (Fabian et al. 2005; Davis et al. 2011); in their works the affinity, quantified by dissociation constant  $K_d$ , was measured using a ATP site-dependent competition binding assay protocol (Fabian et al. 2005). These compiled samples were classified into three groups in terms of the inhibitor category, and each group included at least one member with complex crystal structure available in the PDB database (Berman et al. 2000). The 20 samples are tabulated in Supporting Information (SI) Table S1.

#### *Somatic mutations of EGFR TK domain in TKI-treated NSCLC*

The complete human EGFR protein consists of extracellular domain (EGF binding), transmembrane domain (TM), and intracellular tyrosine kinase (TK) domain and autophosphorylation regions. The TK domain is the functional core of the protein that stretches from exon 18 to exon 24 and its somatic mutations are basically limited to exons 18–21 (residues 687–875). The observed somatic mutations of EGFR in NSCLC are collected in the SM-EGFR-DB database (<http://somaticmutations-egfr.org/index.html>), from which we only selected those of TKI-treated single-point mutations over the EGFR sequence region 687–875. Consequently, a total of 71 EGFR TK mutations were extracted and illustrated in Fig. 1. The mutations are naturally uneven that some residue positions such as E709, G719 and L858 exhibit multiple substitutions, while some others have not yet been observed to have alterations in NSCLC.

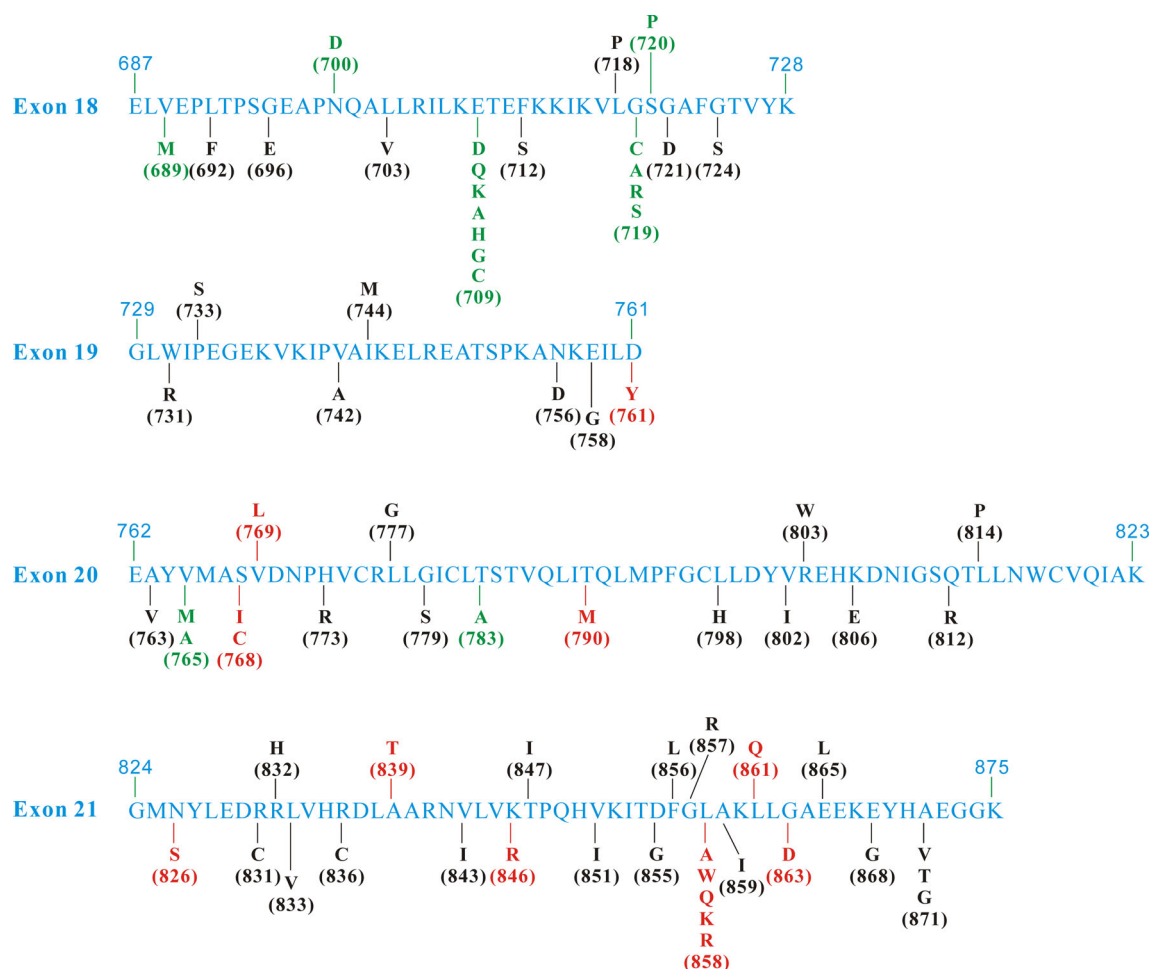


**Fig. 1** The somatic single-point mutations in EGFR TK domain observed in TKI-treated NSCLC; these mutations were retrieved from the SM-EGFR-DB database (<http://somaticmutations-egfr.org/index.html>). The mutations associated with drug resistance and sensitivity

are colored in *red* and *green*, respectively, and those unclear to their impact on drug behavior are in *black* (Riely et al. 2006; Sharma et al. 2007) (color figure online)

#### Collection of representative small-molecule inhibitors that target EGFR TK domain

The EGFR inhibitors can be classified into reversible and irreversible; the former inhibits the tyrosine kinase activity of EGFR by competing with ATP for the ATP-binding site, whereas the latter is covalently bonded to the serine residues nearby the site to disturb EGFR function. In this study, only reversible EGFR inhibitors were investigated (Doebele et al. 2010). Here, we collected six small-molecule inhibitors that target EGFR TK domain, including three FDA-approved drugs, two compounds under clinical development and a natural product, Staurosporine, isolated from the bacterium *Streptomyces staurosporeus* that exhibits wide inhibition on diverse protein kinases (Rüegg and Burgess 1989). All of these selected inhibitors are available to their high-resolution crystal structures in complex with wild-type EGFR (Table 1). In addition, the EGFR natural substrate, ATP, was used as the reference to

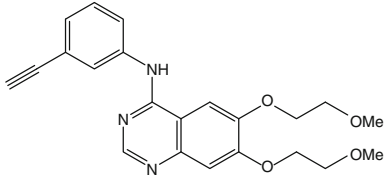
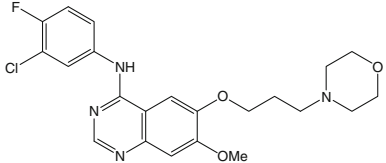
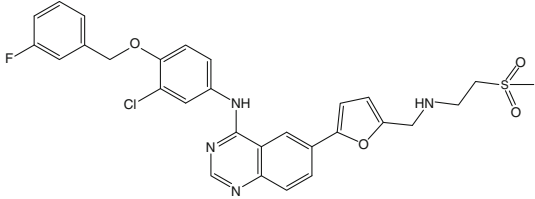
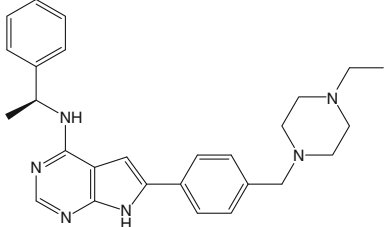
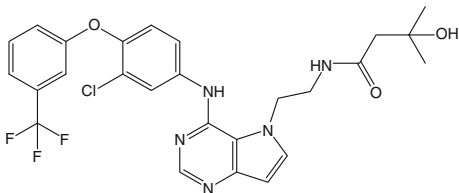
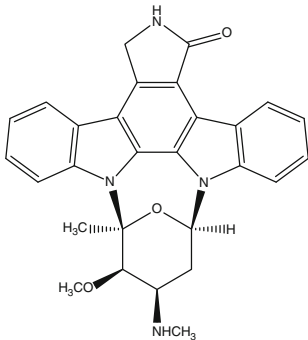
explore competitive inhibition of small-molecule drugs to ATP binding.

#### Computational modeling of EGFR–ligand complex structure

##### Construction of EGFR mutant–inhibitor complex structure model

Although there are a large number of X-ray-solved crystal structures of EGFR and its mutants in complex with diverse small-molecule ligands available in the PDB database (Berman et al. 2000), this is still far from the requirement of this study if considering that we attempted to investigate the systematic interaction profile of all somatic mutations in the EGFR TK domain with a panel of representative inhibitors. In this respect, we employed a computational scheme to construct the structure models of EGFR mutant–inhibitor complexes (Fig. 2a): (i) EGFR–

**Table 1** The six representative EGFR inhibitors

Inhibitor			Complex crystal structure	
Name (generic)	Structure	Status	PDB	EGFR
OSI776 (Erlotinib)		Approved	1M17	Wild type
ZD1839 (Gefitinib)		Approved	2ITY	Wild type
GW572016 (Lapatinib)		Approved	1XKK	Wild type
AEE788		Clinical	2J6M	Wild type
TAK-285		Clinical	3POZ	Wild type
AFN941 (Staurosporine)		Natural product	2ITW	Wild type

inhibitor complex crystal structure was used as template to generate the complex structure models of different EGFR mutants with the same inhibitor. (ii) The side chain of the residue under mutation was manually removed from

the crystal structure, and then a number of new side chain rotamers were added to the residue using the in-house program 2D-Gralab (Zhou et al. 2009a) based on a penultimate rotamer library (Lovell et al. 2000).

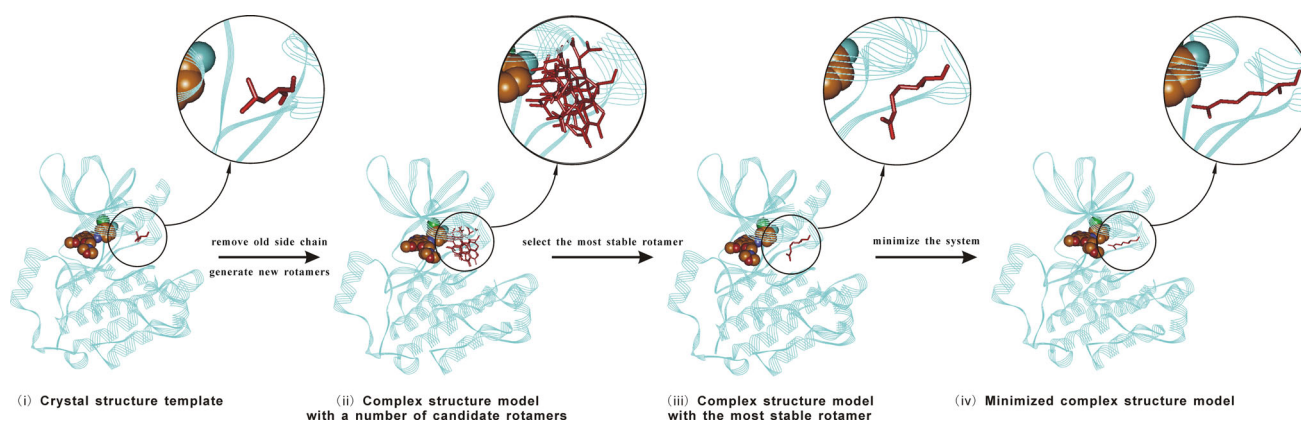


**Fig. 2** Computational modeling of EGFR mutant–inhibitor complex structure from the crystal template of wild-type EGFR in complex with the inhibitor (PDB: 1M17)

(iii) Conformational searching was carried out over these rotamers to pick up the most stable one from the rotamer clusters, where the empirical atomic contact potential (Zhang et al. 1997) was utilized to fast evaluate energetic stability for these rotamers. (iv) The complex system with the selected rotamer was structurally optimized using the AMBER parm03 force field (Duan et al. 2003) implemented in AMBER10 package (Case et al. 2005). In the procedure, the system was successively minimized using 500-step steepest descent and 2,000-step conjugate gradient, the solvent effect was described by implicit generalized Born (GB) model (Bashford and Case 2000), and the force field parameters for the inhibitor molecule were assigned with the generalized amber force field (GAFF) scheme (Wang et al. 2004).

#### Construction of EGFR–ATP complex structure model

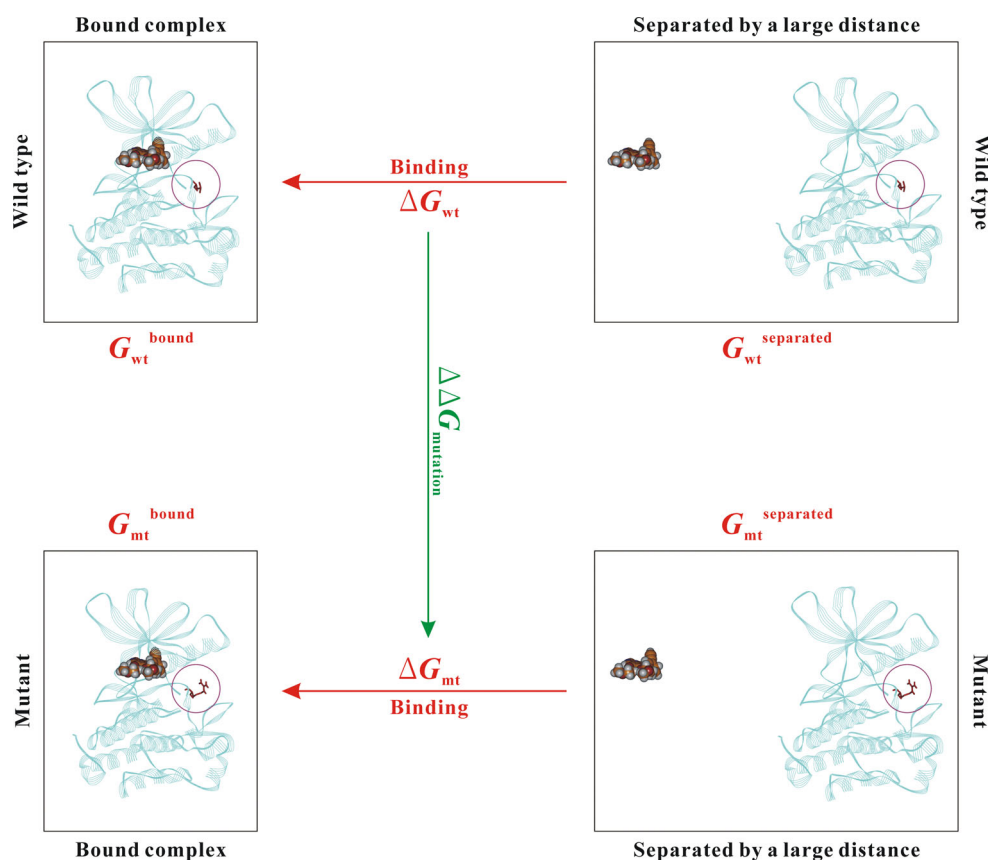
It has been reported that EGFR mutation may cause drug resistance by increasing ATP affinity to the mutant (Yun et al. 2008). Therefore, the interactions between various EGFR mutants and ATP were also investigated in this study. As the complex structure of EGFR (or its mutants) with ATP has not yet been experimentally solved to date, we herein adopted the high-resolution crystal structure of wild-type EGFR bound with AMP-PNP (PDB: 2itx) to model EGFR–ATP complex structure. The AMP-PNP is a non-hydrolyzable analog of ATP, and its only difference to ATP is that a secondary amine moiety, but not a oxygen atom as that in ATP, connects between the first and second phosphates. Thus, the AMP-PNP structure in the crystal template can be readily modified to ATP manually, and then the resulting structure model of EGFR complexed with ATP was subjected to a minimization procedure as described above.

#### Calculation of ligand affinity change upon EGFR mutation

The hybrid quantum mechanics/molecular mechanics (QM/MM) developed by Morokuma and co-workers (Svensson et al. 1996) enables different levels of theory to be applied to different parts of a large system and combined to produce a consistent energy expression. The objective is to perform a high-level calculation on just a small part of the system and to include the effects of the remainder at lower levels of theory, with the end result being a similar accuracy to a high-level calculation on the full system (Alzate-Morales et al. 2009). In recent years, QM/MM has been widely applied to studying biomolecular binding phenomena (Gleeson and Gleeson 2009a), which, for example, was successfully employed to derive scoring function for protein–ligand docking (Hayik et al. 2010), to perform three-dimensional quantitative structure–activity relationship (3D-QSAR) modeling of enzyme inhibitors (Chung et al. 2010), and to explore fragment-based drug design (Gleeson and Gleeson 2009b). Previously, based on the QM/MM methodology, we have described a strategy that enables fast and reliable evaluation of the interaction free energy between protein receptors and small-molecule ligands or peptides (Zhou et al. 2009b). Here, this strategy was further modified to calculate ligand affinity change upon EGFR mutation.

The scheme is schematically illustrated in Fig. 3. First, the complex structures of wild-type EGFR and its mutant with the same inhibitor were modeled using the protocol as described above, and then the QM/MM (in consideration of solvent effects, *vide post*) was utilized to calculate the interaction free energy between the wild-type or mutant EGFR and the inhibitor ( $\Delta G_{wt}$  or  $\Delta G_{mt}$ ); the calculation was accomplished by performing single-point energy

**Fig. 3** The scheme of calculating ligand affinity change  $\Delta\Delta G_{\text{mutation}}$  upon EGFR mutation. The mutated residue is cycled and the inhibitor molecule is shown in *ball* style



computations twice, one on the bound complex system ( $G_{\text{wt}}^{\text{bound}}$  or  $G_{\text{mt}}^{\text{bound}}$ ) and the other on the same system, but its members (EGFR and inhibitor) were separated by a sufficiently large distance from each other ( $G_{\text{wt}}^{\text{separated}}$  or  $G_{\text{mt}}^{\text{separated}}$ ). In this way, the interaction free energy can be approximately expressed as  $\Delta G_{\text{wt}} = G_{\text{wt}}^{\text{bound}} - G_{\text{wt}}^{\text{separated}}$  or  $\Delta G_{\text{mt}} = G_{\text{mt}}^{\text{bound}} - G_{\text{mt}}^{\text{separated}}$ , and the ligand affinity change upon the EGFR mutation was thus derived to be  $\Delta\Delta G_{\text{mutation}} = \Delta G_{\text{mt}} - \Delta G_{\text{wt}}$  (mutation energy). Although we have found that the QM/MM would systematically overestimate protein–ligand interaction energy  $\Delta G$  (Tian et al. 2011a, b), this problem is obviously not the matter in this study because we herein only concerned the relative  $\Delta G$  values before and after the mutation; the systematic bias can be readily eliminated in the final mutation energy  $\Delta\Delta G_{\text{mutation}}$ .

The QM/MM implemented in Gaussian03 suite of programs (Frisch et al. 2003) was used to calculate the free energy  $G$  of bound or separated complex system. In the scheme, the system was partitioned into two layers; the inhibitor molecule and the mutated residue were included in inner layer and treated with a high-level QM theory, while the rest of the system was in outer layer and described using a low-level MM method. For the partitioned system, hydrogen atoms were used as link atoms to saturate the dangling bonds, and the electrostatic interactions between the two layers were treated in terms of

mechanical embedding scheme to save computational cost (Lu et al. 2009). In this study, the semi-empirical AM1, ab initio Hartree–Fock (HF) and density functional theories (DFT) B3LYP and MPWLYP in conjunction with 6-31G+(d) basis set—these four methods have previously been reported to perform QM/MM analysis of protein–ligand systems (Zhou et al. 2009b; Lu et al. 2009; Guo et al. 2012)—were considered in the inner QM layer, and the AMBER force field was used for the outer MM layer. The higher-level theories such as Møller–Plesset perturbation and coupled cluster were not considered here because they are too computationally expensive to perform calculations for the large-scale purpose as in this study. The restricted electrostatic potential (RESP) fitting procedure (Comell et al. 1993) was employed to obtain partial atomic charges of the inhibitor molecule and the non-standard amino acid atoms. Parameters that are not found in standard AMBER force field are defined using the generalized amber force field (GAFF) (Wang et al. 2004). In addition, the solvent effects associated with EGFR–inhibitor binding were described using two empirical methods, i.e. Poisson–Boltzmann/surface area (PB/SA) (Kollman et al. 2000) and additive model (AM) (Eisenberg and McLachlan 1986). The detailed descriptions of PB/SA and AM can be found in our previous publications (Li et al. 2009; Tian et al. 2011a, b), in which we successfully

integrated the two solvent models with QM/MM to investigate protein–ligand interactions.

### EGFR kinase assay

A protocol modified from previous reports (Brignola et al. 2002; Tan et al. 2012; Peng et al. 2013) was used to perform EGFR kinase assay. Briefly, 100- $\mu$ L purified EGFR kinases (2 ng/ $\mu$ L) were diluted in the kinase assay buffer (100-mM Hepes pH 7.5, 4-mM  $\text{MgCl}_2$ , 0.2-mM  $\text{MnCl}_2$ , 0.4-mM sodium orthovanadate, 2-mM DL-dithiothreitol and 0.02 % Triton X-100) containing 30 ng/ $\mu$ L substrate GST-Crk fusion protein, 10- $\mu$ M ATP and 1  $\mu$ Ci [ $\gamma$ - $^{32}$ P]ATP. The mix was incubated with Staurosporine at 0.05, 0.1, 0.25, 0.8, 3, 10, 40 and 160  $\mu$ M on ice for 10 min followed by incubation at 30  $^\circ\text{C}$  for 30 min. The reaction was stopped by the addition of SDS gel loading buffer, the proteins were resolved on SDS-PAGE. The dried gel was then exposed to the PhosphorImager (Molecular Dynamics, Sunnyvale, US) to detect radioactivity. The phosphorylated Crk was plotted against the concentration of Staurosporine to determine  $\text{IC}_{50}$  for kinase inhibition. In this study, the purified proteins of wild-type EGFR as well as its T790M and T790M/L858R mutants were obtained from Sigma-Aldrich Co., Ltd. (Dorset, UK). The GST-Crk were transformed in *Escherichia coli* and purified by glutathione affinity with glutathione-Sepharose 4B beads; GST was the tag used to purify the protein. GST-Crk was removed from the glutathione beads in 10-mM reduced glutathione in 50-mM Tris-HCl (pH 8.0).

## Results and discussion

### Optimization of QM/MM-solvent model combination for the EGFR–inhibitor system

Previously, different levels of QM theory ranging from semi-empirical, to ab initio and to DFT have been employed to carry out QM/MM calculations of protein–ligand interaction, and also different solvent models were coupled with the QM/MM to account for associated desolvation effects. However, it is unclear which kinds of theory and model are most applicable for the current EGFR–inhibitor system. In this respect, we herein performed a systematic examination of four sophisticated QM theories (AM1, HF, B3LYP and MPWLYP) and two empirical solvent models (PB/SA and AM) to determine the optimal combination of theory and model in reproducing interaction free energy involved in the system. The examination was carried out on the basis of 20 experimentally measured affinity values ( $\text{pK}_d$ ) of 3 FDA-approved drugs to a variety of wild-type and mutant EGFR (SI Table S1). These experimental values were compared to

interaction free energies ( $\Delta G$ ) calculated using the eight combinations between the four QM theories and the two solvent models.

As can be seen in Fig. 4a–h, the  $\Delta G$  calculated by the eight combined methods all exhibit negative correlation with experimental  $\text{pK}_d$ . This is expected because high affinity is always associated with a significant decrease in total free energy of the system upon EGFR–inhibitor binding. The Pearson's coefficients  $R_{\text{Pearson}}$  vary considerably over different combinations, ranging from the lowest  $-0.257$  (HF/AMBER + AM) to the highest  $-0.692$  (MPWLYP/AMBER + PB/SA). In addition, from the histogram representation of  $R_{\text{Pearson}}$  (Fig. 4i), it is evident that QM theories have a dominant influence on the final calculated results as compared to solvent models, and the latter only casts a modest effect on the resulting  $R_{\text{Pearson}}$  for different method combinations. The DFT functional MPWLYP seems to perform much well in estimating EGFR–inhibitor binding affinity, its coupling with PB/SA solvent model can achieve the best result for the system ( $R_{\text{Pearson}} = -0.692$ ). In fact, the MPWLYP functional has been testified to provide accuracies close to high-level electronically correlated methods in recent study of biomolecular recognition (Lu et al. 2009; Zhou et al. 2009b), and it is therefore not surprising that this method can give satisfactory result for characterizing the interaction energy of EGFR with inhibitor. Unexpectedly, the ab initio HF performed much worse than the semi-empirical AM1, but this is also reasonable because the electronic correlation properties important for the weak non-bonded interactions of protein–ligand complex are completely neglected by the HF, but these properties are implicitly involved in the experimental data utilized to parameterize AM1 method. The B3LYP functional, although it is very popular in the theoretical biochemistry community, appears not to be a good choice for studying the EGFR–inhibitor binding phenomenon, which only shows a moderate correlation with experimental affinities over the 20 samples ( $R_{\text{Pearson}} = \sim -0.5$ ).

It is worth noting that the calculated interaction energies  $\Delta G$  of EGFR with inhibitors vary from  $-60$  to  $-20$  kcal/mol; obviously the values were overestimated with respect to experimental binding affinities  $K_d$ , which are at nanomole level (1–100 nM), corresponding to free energy changes of  $\sim -10$  kcal/mol ( $\Delta G = -RT \ln 1/K_d$ ). In fact, in an early study, we found that the protein–ligand binding potencies derived from QM/MM analysis involve strong systematic bias that represents a significant difference between the absolute values of calculated and experimental results—this is not unexpected considering that some secondary factors such as conformational entropy and strain energy incurred from the binding may not be taken into account in the calculated results (Fu et al. 2011; Polyansky et al. 2012). However, the QM/MM method can indeed

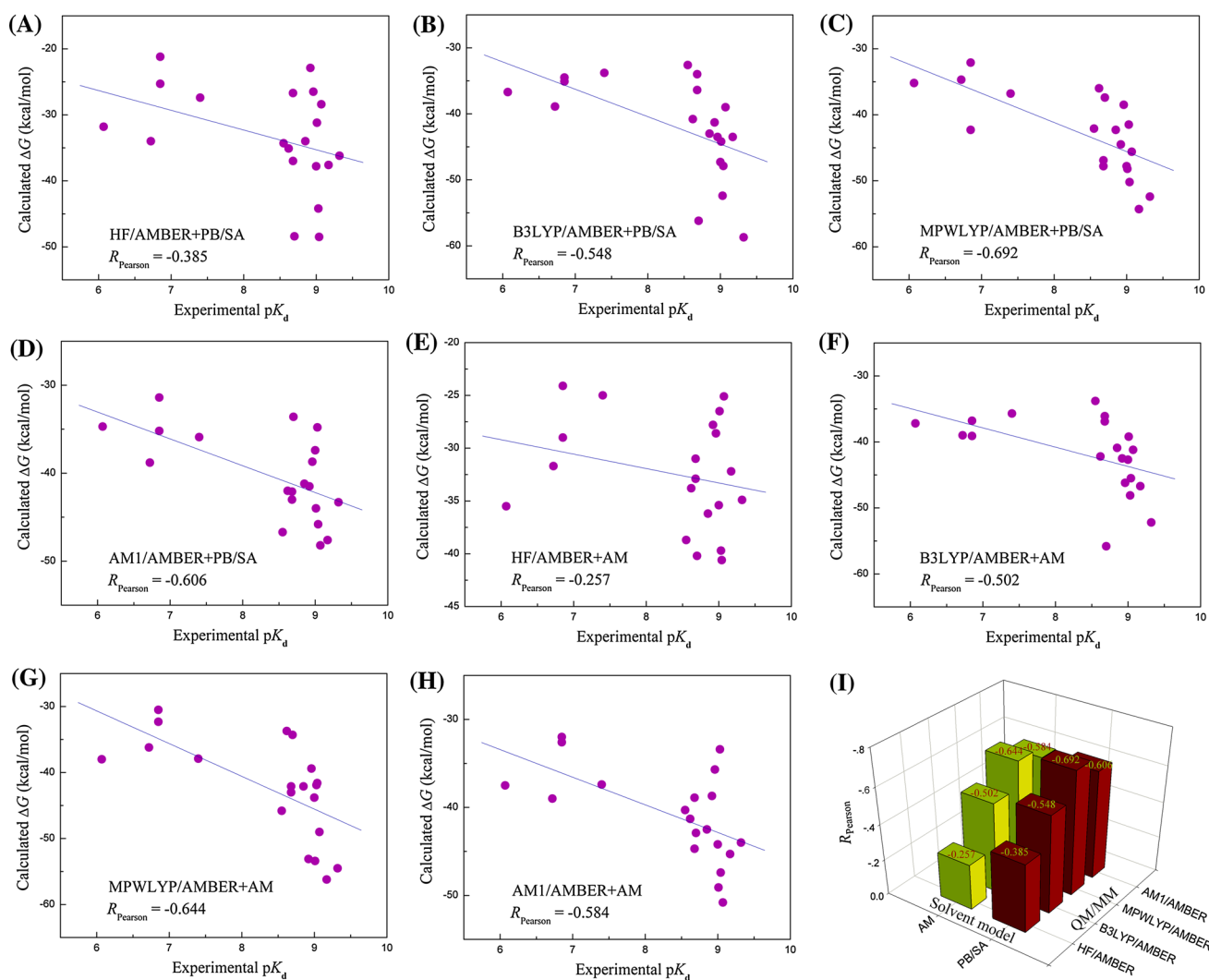


**Fig. 4** Scatter plots of experimental affinity  $pK_d$  against interaction free energy  $\Delta G$  calculated using different combinations of QM/MM methods and solvent models: **a** HF/AMBER + PB/SA, **b** B3LYP/AMBER + PB/SA, **c** MPWLYP/AMBER + PB/SA, **d** AM1/AMBER + PB/SA, **e** HF/AMBER + AM, **f** B3LYP/AMBER +

AM, **g** MPWLYP/AMBER + AM and **h** AM1/AMBER + AM. The data of calculated interaction free energies are listed in SI Table S1. **i** Histogram representation of the Pearson's correlation coefficients  $R_{\text{Pearson}}$  obtained from the different combinations of QM/MM methods and solvent models

give a proper prediction for the relative free change upon EGFR–inhibitor binding, as demonstrated by a good linear correlation between the calculated  $\Delta G$  and experimental  $pK_d$ . In this regard, it is apparent that the systematic bias involved in QM/MM-derived free energies  $\Delta G$  can be readily eliminated for the mutation energy  $\Delta\Delta G_{\text{mutation}}$  concerned in this study, which is expressed as the difference in EGFR–inhibitor interaction energy before and after the mutation, viz.  $\Delta\Delta G_{\text{mutation}} = \Delta G_{\text{mt}} - \Delta G_{\text{wt}}$ .

#### Systematic analysis of inhibitor affinity changes upon various EGFR mutations

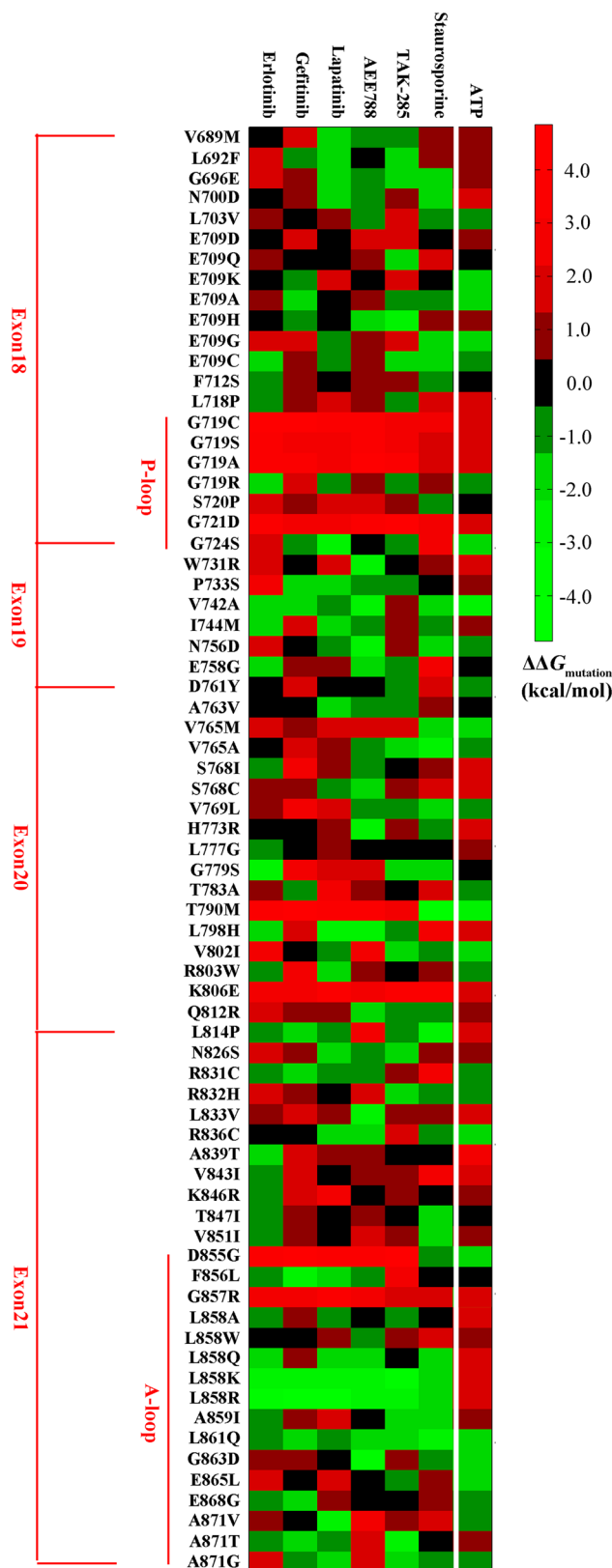
The optimal combination of MPWLYP/AMBER and PB/SA (MPWLYP/AMBER + PB/SA) was employed to

calculate one by one the mutation energies  $\Delta\Delta G_{\text{mutation}}$  associated with the 497 terms of 7 ligands (6 inhibitors plus substrate ATP) against 71 somatic EGFR mutations. This is an exhaustive procedure but can give a sufficiently accurate estimation for the systematic profile of clinical inhibitors responsive to various EGFR mutations. The calculated results are shown as a heat map in Fig. 5 (the data are provided in SI Table 2), in which the green, red and black colors represent favorable, unfavorable and neutral mutations, respectively. As can be seen, most mutations have a modest/moderate influence on inhibitor affinity to EGFR ( $-2 \text{ kcal/mol} < \Delta\Delta G_{\text{mutation}} < 2 \text{ kcal/mol}$ ), and only few exert large efficacy to the affinity ( $\Delta\Delta G_{\text{mutation}} > 3 \text{ kcal/mol}$  or  $< -3 \text{ kcal/mol}$ ). We have examined the relationship between the location of mutations in EGFR protein

**Fig. 5** The heat map representation of the mutation energy profile of 7 ligands (6 inhibitors plus substrate ATP) against 71 somatic mutations in EGFR. The data are provided in SI Table S2. The *green*, *red* and *black* colors represent favorable, unfavorable and neutral mutations, respectively (color figure online)

architecture and its impact on inhibitor binding, and found that most somatic mutations in EGFR are far away from the ATP-binding site of EGFR and also these mutations contribute limitedly to the mutation energy. This is in line with the fact that only very few mutations such as L858R, G719S and T790M were observed to have a large effect on inhibitor interaction with EGFR.

As expected, the L858R, G719S and T790M mutations are located around EGFR ATP-binding site and thus can directly reshape the geometric and physiochemical properties of the site (Fig. 6a). The L858R and G719S confer constitutive activation to the kinase and have been reported to sensitize EGFR inhibitors (Yun et al. 2007; Yoshikawa et al. 2013). According to our calculations, the L858R, and its analog L858K, can considerably promote inhibitor binding to EGFR by enhancing their interaction free energies with  $\sim 3$  kcal/mol over the six investigated inhibitors. However, the G719S and its several analogs such as G719C and G719A do not directly increase inhibitor affinity; in fact, the interaction free energies between EGFR and inhibitors were calculated to decrease by  $\sim 2$  kcal/mol associated with these mutations. Interestingly, Yun et al. (2007) have quantitatively assayed the binding of anti-lung cancer drug Gefitinib to wild-type and G719S mutant EGFR and found a twofold decrease in the binding affinity due to the mutation ( $K_d$  increases from 53.5 to 123.6 nM). In addition, another important mutation in EGFR is T790M, which has been reported to be closely associated with acquired resistance in TKI-treated NSCLC (Ma et al. 2011). The threonine 790 is the “gatekeeper” residue, an important determinant of inhibitor specificity in the ATP-binding site. Previous experimental evidences suggested that the increased ATP affinity is a primary mechanism by which the T790M mutation confers drug resistance (Yun et al. 2008)—this can be well reflected in the calculated mutation energy profile (Fig. 5), where the T790M renders a considerable improvement in ATP affinity to EGFR ( $\Delta\Delta G_{\text{mutation}} = -2.38$  kcal/mol). Moreover, we also found that this mutation will significantly lower the interaction free energy of EGFR with different inhibitors ( $\Delta\Delta G_{\text{mutation}} = \sim 3$  kcal/mol) and, in this way, impair drug sensitivity to NSCLC. Previously, Yun et al. (2008) reported that the T790M mutant binds Gefitinib with a higher nanomolar affinity as compared to wild-type EGFR ( $K_d$  decreases from 35.3 to 4.6 nM), but in a later study the same mutation was measured by Davis et al. (2011) to largely decrease Gefitinib affinity ( $K_d$  increases



from 1 to 40 nM). Obviously, our calculations supported the findings of Davis et al., and we therefore concluded that the observed drug resistance associated with the T790M

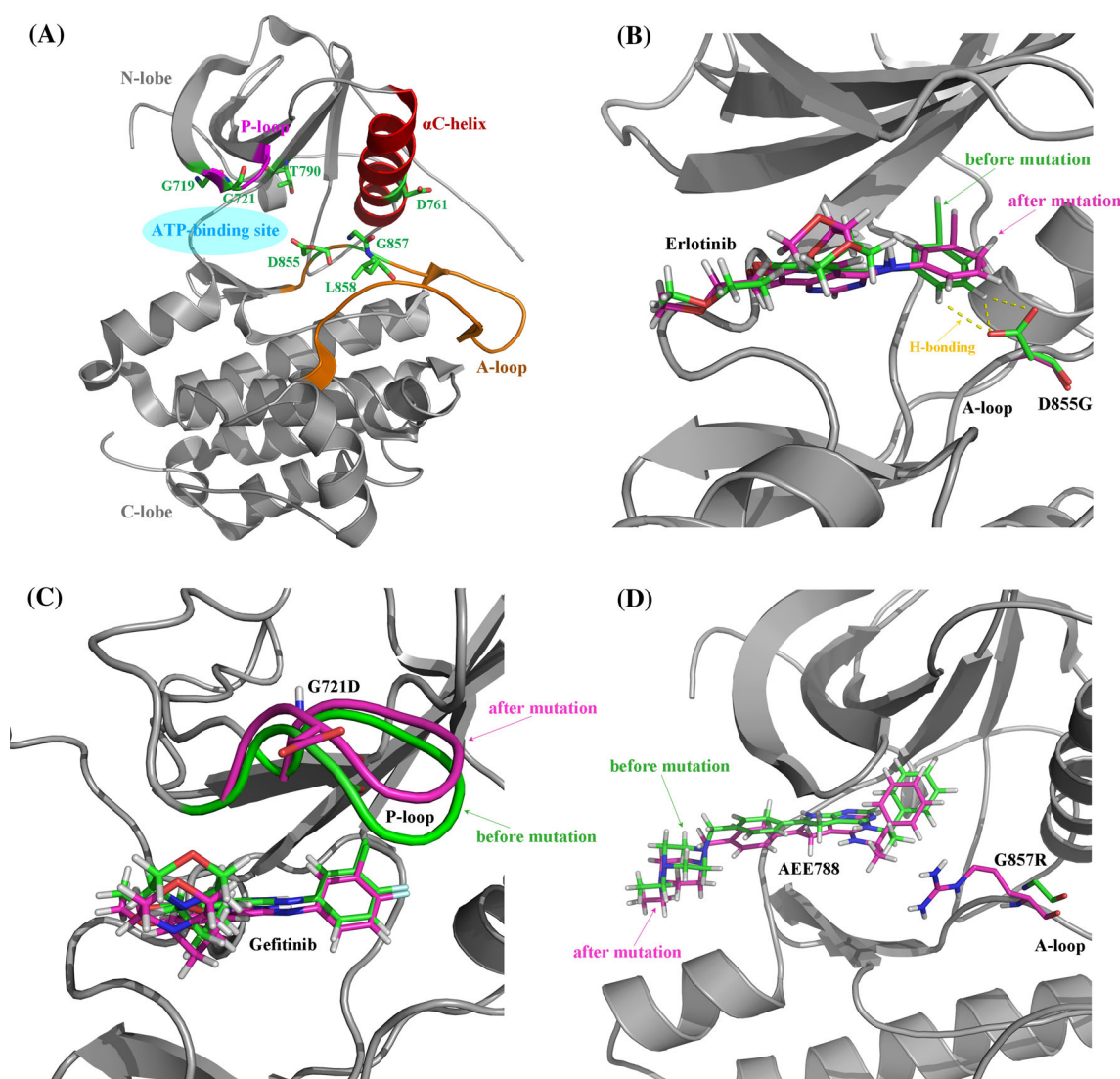


**Fig. 6** **a** Stereoview of EGFR structure architecture (PDB: 2J6M). **b–d** The local structure variations around bound inhibitor molecules Erlotinib, Gefitinib and AEE788 upon EGFR residue mutations D855G, G721D and G857R, respectively

mutation is a co-effect of increasing ATP affinity and decreasing inhibitor affinity.

Balak et al. (2006) have found a rare secondary D761Y mutation in EGFR isolated from lung adenocarcinomas that can also cause acquired resistance to kinase inhibitors. According to our analysis, however, this mutation does not substantially influence the intermolecular interaction between EGFR and inhibitors ( $\Delta\Delta G_{\text{mutation}} = \sim 1$  kcal/mol). This can be solidified by visually examining EGFR structure architecture; it is seen from Fig. 6a that the residue 761 is located at the N-lobe  $\alpha$ C-helix of EGFR TK domain, apart from the ATP-binding site more than 15 Å, which can thus only exert a limited effect on inhibitor binding. In this respect, it is suggested that the D761Y-associated drug resistance may be acquired through some bypass pathways such as altering EGFR–cellular

machinery interaction and/or shifting EGFR signaling network (Hopper-Borge et al. 2009), rather than by directly impairing inhibitor affinity.

Identification of potential EGFR mutations that might cause drug resistance

From the mutation energy profile it is seen that there are few EGFR mutations including D855G, G721D and G857R that can address a consistent unfavorable effect on inhibitor binding and thus are the potential candidates to cause acquired resistance in lung cancer to kinase inhibitors. These three mutations are located around the ATP-binding site (Fig. 6a) and may generically lower drug affinity to EGFR by direct non-bonded approach or indirect allosteric effect, albeit they are not frequently observed. To

gain a clear picture about the structural details of these potential resistance-associated mutations, we herein performed a QM/MM minimization to fully optimize the structure architecture of inhibitors complexed with these EGFR mutants. In the procedure, the inhibitor molecule and the mutated residue are included in QM layer, while the rest of the complex system is in MM layer, and the resulting structure models superposed between the wild-type and mutant EGFR bound with inhibitors are shown in Fig. 6b–d.

#### D855G mutation

The D855 residue is an intrinsic component of the ATP-binding site and directly contacts bound ligand molecule. In the wild-type EGFR–Erlotinib complex system (PDB: 1M17), the negatively charged carboxyl group of D855 can form a number of hydrogen bonding (H bonding) and electrostatic interactions with the hydrogen atoms in the phenyl moiety of Erlotinib molecule, donating substantial affinity contribution to the complex. The D855G mutation removes the side chain of D855 and breaks these stabilization interactions between the D855 and inhibitor (Fig. 6b), rendering a considerable free energy loss in the system ( $\Delta\Delta G_{\text{mutation}} = 3.97$  kcal/mol). In addition, the D855G leads to a moderate motion of Erlotinib in the ATP-binding site, which weakens the interaction of ligand molecule with the EGFR A-loop. Although the D855G is unfavorable to inhibitor binding, it appears to stabilize EGFR–ATP complex with a free energy income of  $\Delta\Delta G_{\text{mutation}} = -2.06$  kcal/mol. This can be explained by the fact that the mutation eliminates the electrostatic repulsion between the negatively charged groups of EGFR D855 residue and ATP phosphate. In this regard, D855G mutation is expected to cause drug resistance by simultaneously decreasing inhibitor affinity and increasing ATP affinity, which is very similar to the T790M mutation.

#### G721D and G857R mutations

The residue G721 is located at the P-loop of EGFR but does not directly contact inhibitor molecule. In fact, the mutation of neutral glycine to charged aspartic acid at this position can largely modify the local chemical environment around the residue 721, leading to a significant conformational change in the P-loop, which considerably weakens the interaction stability of inhibitors with EGFR ( $\Delta\Delta G_{\text{mutation}} = \sim 3$  kcal/mol) (Fig. 6c). Interestingly, the conformational change in P-loop also addresses unfavorable effect on ATP binding, with free energy penalty of  $\Delta\Delta G_{\text{mutation}} = 2.06$  kcal/mol.

The residue G857 is at the A-loop of EGFR and separated from the ATP-binding site by a 5 Å distance.

Previous works reported that its neighboring mutation L858R stabilizes EGFR–inhibitor system (Yun et al. 2007), but according to our calculations the G857R would cause moderate affinity loss for inhibitor binding ( $\Delta\Delta G_{\text{mutation}} = 1\text{--}2$  kcal/mol) via associated structural motions in A-loop and inhibitor molecule (Fig. 6d); the mutation also impairs EGFR interaction with ATP by a destabilization energy of  $\Delta\Delta G_{\text{mutation}} = 1.87$  kcal/mol.

Overall, the G721D and G857R mutations destabilize the complex systems of EGFR with both the inhibitors and ATP. Hence, it is unclear whether they can significantly influence the inhibitory activity of drug entities to the mutant EGFR due to the competitive mechanism between inhibitors and ATP for the ATP-binding site.

In silico analysis and in vitro assay of staurosporine sensitivity to EGFR mutations

The first-generation EGFR targeting agents are reversible kinase inhibitors such as Gefitinib and Erlotinib, which were reported to be sensitive to the L858R mutant that confers constitutive activation for the EGFR kinase in NSCLC (Siegel-Lakshai et al. 2005). However, these drugs exhibit strong resistance to the secondary mutation T790M in EGFR; the T790M has generally been considered to be an acquired mutation, found in 40–50 % of cases at the time of clinical progression to the Gefitinib or Erlotinib (Rosell et al. 2011). Although a number of irreversible inhibitors have been developed to overcome acquired resistance associated with the T790M mutation (Zhou et al. 2009c; Takezawa et al. 2010; Carmi et al. 2012), these suicide substances show high side effect and low selectivity that limit their clinical practice. Therefore, design of new reversible EGFR inhibitors with high affinity to T790M mutant is of great interest in the medicinal chemistry community.

Here, we in silico analyzed the interaction profile of various EGFR mutants with the Staurosporine, a natural product that was originally isolated from the bacterium *Streptomyces staurosporeus* and possesses wide inhibitory potency on diverse protein kinases (Rüegg and Burgess 1989). According to our calculations, the Staurosporine has relatively low interaction energy with wild-type EGFR, but it would receive a large free energy income ( $\Delta\Delta G_{\text{mutation}} = -4.83$  kcal/mol) due to the T790M mutation. This is quite different to those traditional reversible EGFR inhibitors that generally have lower affinity to the T790M mutant than wild-type EGFR. Further, we examined the complex structure model of Staurosporine with the mutant and found that the mutated M790 residue can form intensive hydrophobic forces and S $\cdots\pi$  interactions with, respectively, the aromatic ring and amide moiety of Staurosporine, contributing considerable stabilization energy to

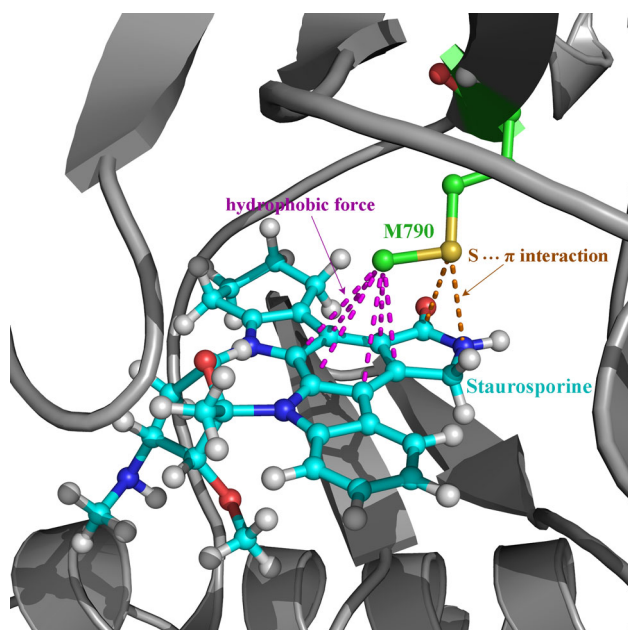


**Fig. 7** The S... $\pi$  interaction and hydrophobic force formed between the Staurosporine and M790 residue in T790M mutant EGFR

**Table 2** The calculated mutation energy  $\Delta\Delta G_{\text{mutation}}$  and experimental inhibitory activity  $IC_{50}$  of Staurosporine to wild-type EGFR and its T790M, L858R and T790M/L858R mutants

EGFR	Calculated $\Delta\Delta G_{\text{mutation}}$ (kcal/mol)	Experimental $IC_{50}$ (nM)
Wild type	0.0	$937 \pm 86^a$
T790M	-4.83	$12 \pm 2.3^a$
L858R	-0.78	— <sup>b</sup>
T790M/L858R	-5.09	$3 \pm 0.9^a$

<sup>a</sup> For duplicate

<sup>b</sup> Not assayed

the complex system (Fig. 7). In addition, the removal of hydroxyl group in native T790 residue associated with the mutation may eliminate some unfavorable polar interactions in the wild-type system. To verify this theoretical supposition, we have performed in vitro kinase assay to measure the inhibitory activity of Staurosporine against wild-type and T790M mutant EGFR; the obtained  $IC_{50}$  values are listed in Table 2. It is encouraged that Staurosporine exhibits a 80-fold higher inhibitory efficacy on T790M mutant over wild-type EGFR ( $IC_{50} = 12$  and  $937$  nM, respectively). Moreover, the mutation energies  $\Delta\Delta G_{\text{mutation}}$  of Staurosporine upon L858R and dual T790M/L858R mutations were estimated to be  $-0.78$  and  $-5.09$  kcal/mol, respectively, suggesting that Staurosporine has a relatively low sensitivity to the L858R mutant, but the combination of L858R and T790M mutations, which is very common in acquired resistance of

NSCLC, will significantly improve the sensitivity. The computational finding can be readily confirmed with the kinase assay experiment by which the  $IC_{50}$  value of Staurosporine to the dual T790M/L858R mutant was measured to be  $3$  nM (Table 2), which represents a very high inhibitory activity if considering that the  $IC_{50}$  values of clinical drugs Gefitinib and Erlotinib against their cognate L858R mutant are only  $80$  and  $40$  nM, respectively (Costa et al. 2008). In this regard, the Staurosporine is suggested as a promising lead compound from which investigators can design and optimize new reversible inhibitors with high potency and selectivity to target drug-resistant EGFR mutants.

## Conclusions

EGFR mutations were reported to cause both drug resistance and sensitivity to small-molecule tyrosine kinase inhibitors. Understanding of the molecular mechanism and biological implication underlying drug response to the mutations is fundamentally important for design of new anti-cancer agents with high potency and selectivity to target drug-resistant mutants. In this study, we have systematically investigated the complete profile of several representative EGFR inhibitors in response to various EGFR mutations using a combined QM/MM-PB/SA scheme. The calculated mutation energy profile imparted that most observed somatic mutations in EGFR TK domain are far away from the ATP-binding site and thus only cast limited effect on inhibitor binding, while few mutated residues that are located around the site can substantially impact the binding by directly breaking the non-bonded interaction of EGFR with inhibitors or by indirectly addressing allosteric effect on the kinase. In particular, the “gatekeeper” mutation T790M was suggested to increase ATP affinity and decrease inhibitor affinity simultaneously, whereas another rare secondary mutation D761Y appeared not to directly influence EGFR–inhibitor interaction. We also identified several potential mutations including G721D, D855G and G857R that might cause drug resistance for most investigated inhibitors. In addition, the natural kinase blocker Staurosporine was found to have a low sensitivity to wild-type EGFR and its L858R mutant, but a high inhibitory activity against the T790M and T790M/L858R mutants; this compound could be considered as a promising lead entity to develop new reversible EGFR inhibitors combating drug resistance associated with the acquired T790M mutation.

**Conflict of interest** The authors declare that they have no conflict of interest.

## References

- Alzate-Morales JH, Caballero J, Vergara Jague A, González Nilo FD (2009) Insights into the structural basis of N2 and O6 substituted guanine derivatives as cyclin-dependent kinase 2 (CDK2) inhibitors: prediction of the binding modes and potency of the inhibitors by docking and ONIOM calculation. *J Chem Inf Model* 49:886–899
- Balak MN, Gong Y, Riely GJ, Somwar R, Li AR, Zakowski MF, Chiang A, Yang G, Ouerfelli O, Kris MG, Ladanyi M, Miller VA, Pao W (2006) Novel D761Y and common secondary T790M mutations in epidermal growth factor receptor-mutant lung adenocarcinomas with acquired resistance to kinase inhibitors. *Clin Cancer Res* 12:6494–6501
- Bashford D, Case DA (2000) Generalized born models of macromolecular solvation effects. *Annu Rev Phys Chem* 51:129–152
- Berman HM, Westbrook J, Feng Z, Gilliland G, Bhat TN, Weissig H, Shindyalov IN, Bourne PE (2000) The protein data bank. *Nucleic Acids Res* 28:235–242
- Brignola PS, Lackey K, Kadwell SH, Hoffman C, Horne E, Carter HL, Stuart JD, Blackburn K, Moyer MB, Alligood KJ, Knight WB, Wood ER (2002) Comparison of the biochemical and kinetic properties of the type I receptor tyrosine kinase intracellular domains. Demonstration of differential sensitivity to kinase inhibitors. *J Biol Chem* 277:1576–1585
- Carmi C, Galvani E, Vacondio F, Rivara S, Lodola A, Russo S, Aiello S, Bordini F, Costantino G, Cavazzoni A, Alfieri RR, Ardizzone A, Petronini PG, Mor M (2012) Irreversible inhibition of epidermal growth factor receptor activity by 3-aminopropanamides. *J Med Chem* 55:2251–2264
- Case DA, Cheatham TE 3rd, Darden T, Gohlke H, Luo R, Merz KM Jr, Onufriev A, Simmerling C, Wang B, Woods RJ (2005) The Amber biomolecular simulation programs. *J Comput Chem* 26:1668–1688
- Chung JY, Chung HW, Cho SJ, Hah JM, Cho AE (2010) QM/MM based 3D QSAR models for potent B-Raf inhibitors. *J Comput Aided Mol Des* 24:385–397
- Comell WD, Cieplak P, Bayly CI, Kollman PA (1993) Application of RESP charges to calculate conformational energies, hydrogen bond energies, and free energies of solvation. *J Am Chem Soc* 115:9620–9631
- Costa DB, Schumer ST, Tenen DG, Kobayashi S (2008) Differential responses to erlotinib in epidermal growth factor receptor (EGFR)-mutated lung cancers with acquired resistance to gefitinib carrying the L747S or T790M secondary mutations. *J Clin Oncol* 26:1182–1184
- Davis MI, Hunt JP, Herrgard S, Ciceri P, Wodicka LM, Pallares G, Hocker M, Treiber DK, Zarrinkar PP (2011) Comprehensive analysis of kinase inhibitor selectivity. *Nat Biotechnol* 29:1046–1051
- Doebbele RC, Oton AB, Peled N, Camidge DR, Bunn PA Jr (2010) New strategies to overcome limitations of reversible EGFR tyrosine kinase inhibitor therapy in non-small cell lung cancer. *Lung Cancer* 69:1–12
- Duan Y, Wu C, Chowdhury S, Lee MC, Xiong G, Zhang W, Yang R, Cieplak P, Luo R, Lee T, Caldwell J, Wang J, Kollman P (2003) Point-charge force field for molecular mechanics simulations of proteins. *J Comput Chem* 24:1999–2012
- Eisenberg D, McLachlan AD (1986) Solvation energy in protein folding and binding. *Nature* 319:199–203
- Fabian MA, Biggs WH 3rd, Treiber DK, Atteridge CE, Azimioara MD, Benedetti MG, Carter TA, Ciceri P, Edeen PT, Floyd M, Ford JM, Galvin M, Gerlach JL, Grotzfeld RM, Herrgard S, Insko DE, Insko MA, Lai AG, Lélis JM, Mehta SA, Milanov ZV, Velasco AM, Wodicka LM, Patel HK, Zarrinkar PP, Lockhart DJ (2005) A small molecule–kinase interaction map for clinical kinase inhibitors. *Nat Biotechnol* 23:329–336
- Frisch MJ, Trucks GW, Schlegel HB, Scuseria GE, Robb MA, Cheeseman JR, Zakrzewski VG, Montgomery JA Jr, Stratmann RE, Burant JC, Dapprich S, Millam JM, Daniels AD, Kudin KN, Strain MC, Farkas O, Tomasi J, Barone V, Cossi M, Cammi R, Mennucci B, Pomelli C, Adamo C, Clifford S, Ochterski J, Petersson GA, Ayala PY, Cui Q, Morokuma K, Malick DK, Rabuck AD, Raghavachari K, Foresman JB, Cioslowski J, Ortiz JV, Stefanov BB, Liu G, Liashenko A, Piskorz P, Komaromi I, Gomperts R, Martin RL, Fox DJ, Keith T, Al-Laham MA, Peng CY, Nanayakkara A, Gonzalez C, Challacombe M, Gill PMW, Johnson BG, Chen W, Wong MW, Andres JL, Head-Gordon M, Replogle ES, Pople JA (2003) Gaussian 03. Gaussian Inc., Wallingford
- Fu Z, Li X, Merz KM Jr (2011) Accurate assessment of the strain energy in a protein-bound drug using QM/MM X-ray refinement and converged quantum chemistry. *J Comput Chem* 32:2587–2597
- Gleeson MP, Gleeson D (2009a) QM/MM calculations in drug discovery: a useful method for studying binding phenomena? *J Chem Inf Model* 49:670–677
- Gleeson MP, Gleeson D (2009b) QM/MM as a tool in fragment based drug discovery. A cross-docking, rescoring study of kinase inhibitors. *J Chem Inf Model* 49:1437–1448
- Guo X, He D, Liu L, Kuang R, Liu L (2012) Use of QM/MM scheme to reproduce macromolecule–small molecule noncovalent binding energy. *Comput Theor Chem* 991:134–140
- Hayik SA, Dunbrack R Jr, Merz KM Jr (2010) A mixed QM/MM scoring function to predict protein–ligand binding affinity. *J Chem Theory Comput* 6:3079–3091
- Hopper-Borge EA, Nasto RE, Ratushny V, Weiner LM, Golemis EA, Astsurov I (2009) Mechanisms of tumor resistance to EGFR-targeted therapies. *Expert Opin Ther Targets* 13:339–362
- Kollman PA, Massova I, Reyes C, Kuhn B, Huo SH, Chong L, Lee M, Duan Y, Wang W, Donini O, Cieplak P, Srinivasan J, Case DA, Cheatham TE (2000) Calculating structures and free energies of complex molecules: combining molecular mechanics and continuum models. *Acc Chem Res* 33:889–897
- Li Y, Yang Y, He P, Yang Q (2009) QM/MM study of epitope peptides binding to HLA-A\*0201: the roles of anchor residues and water. *Chem Biol Drug Des* 74:611–618
- Lin L, Bivona TG (2012) Mechanisms of resistance to epidermal growth factor receptor inhibitors and novel therapeutic strategies to overcome resistance in NSCLC patients. *Chemother Res Pract* 2012:817297
- Lovell SC, Word JM, Richardson JS, Richardson DC (2000) The penultimate rotamer library. *Proteins* 40:389–408
- Lu Y, Shi T, Wang Y, Yang H, Yan X, Luo X, Jiang H, Zhu W (2009) Halogen bonding—a novel interaction for rational drug design. *J Med Chem* 52:2854–2862
- Ma C, Wei S, Song Y (2011) T790M and acquired resistance of EGFR TKI: a literature review of clinical reports. *J Thorac Dis* 3:10–18
- Ohashi K, Maruvka YE, Michor F, Pao W (2013) Epidermal growth factor receptor tyrosine kinase inhibitor-resistant disease. *J Clin Oncol* 31:1070–1080
- Peng YH, Shiao HY, Tu CH, Liu PM, Hsu JT, Amancha PK, Wu JS, Coumar MS, Chen CH, Wang SY, Lin WH, Sun HY, Chao YS, Lyu PC, Hsieh HP, Wu SY (2013) Protein kinase inhibitor design by targeting the Asp-Phe-Gly (DFG) motif: the role of the DFG motif in the design of epidermal growth factor receptor inhibitors. *J Med Chem* 56:3889–3903
- Polyansky AA, Zubac R, Zagrovic B (2012) Estimation of conformational entropy in protein–ligand interactions: a computational perspective. *Methods Mol Biol* 819:327–353

- Prenzel N, Fischer OM, Streit S, Hart S, Ullrich A (2001) The epidermal growth factor receptor family as a central element for cellular signal transduction and diversification. *Endocr Relat Cancer* 8:11–31
- Riely GJ, Politi KA, Miller VA, Pao W (2006) Update on epidermal growth factor receptor mutations in non-small cell lung cancer. *Clin Cancer Res* 12:7232–7241
- Rosell R, Molina MA, Costa C, Simonetti S, Gimenez-Capitan A, Bertran-Alamillo J, Mayo C, Moran T, Mendez P, Cardenal F, Isla D, Provencio M, Cobo M, Insa A, Garcia-Campelo R, Reguart N, Majem M, Viteri S, Carcereny E, Porta R, Massuti B, Queralt C, de Aguirre I, Sanchez JM, Sanchez-Ronco M, Mate JL, Ariza A, Benlloch S, Sanchez JJ, Bivona TG, Sawyers CL, Taron M (2011) Pretreatment EGFR T790M mutation and BRCA1 mRNA expression in erlotinib-treated advanced non-small-cell lung cancer patients with EGFR mutations. *Clin Cancer Res* 17:1160–1168
- Rüegg UT, Burgess GM (1989) Staurosporine, K-252 and UCN-01: potent but nonspecific inhibitors of protein kinases. *Trends Pharm Sci* 10:218–220
- Sharma SV, Bell DW, Settleman J, Haber DA (2007) Epidermal growth factor receptor mutations in lung cancer. *Nat Rev Cancer* 7:169–181
- Shigematsu H, Gazdar AF (2006) Somatic mutations of epidermal growth factor receptor signaling pathway in lung cancers. *Int J Cancer* 118:257–262
- Siegel-Lakshai WS, Beijnen JH, Schellens JH (2005) Current knowledge and future directions of the selective epidermal growth factor receptor inhibitors erlotinib (Tarceva) and gefitinib (Iressa). *Oncologist* 10:579–589
- Svensson M, Humbel S, Froese RDJ, Matsubara T, Sieber S, Morokuma K (1996) ONIOM: a multilayered integrated MO + MM method for geometry optimizations and single point energy predictions. A test for Diels–Alder reactions and Pt(P(t-Bu)(3))(2) + H-2 oxidative addition. *J Phys Chem* 100:19357–19363
- Takezawa K, Okamoto I, Tanizaki J, Kuwata K, Yamaguchi H, Fukuoka M, Nishio K, Nakagawa K (2010) Enhanced anticancer effect of the combination of BIBW2992 and thymidylate synthase-targeted agents in non-small cell lung cancer with the T790M mutation of epidermal growth factor receptor. *Mol Cancer Ther* 9:1647–1656
- Tan F, Shen X, Wang D, Xie G, Zhang X, Ding L, Hu Y, He W, Wang Y, Wang Y (2012) Icotinib (BPI-2009H), a novel EGFR tyrosine kinase inhibitor, displays potent efficacy in preclinical studies. *Lung Cancer* 76:177–182
- Tian F, Yang L, Lv F, Luo X, Pan Y (2011a) Why OppA protein can bind sequence-independent peptides? A combination of QM/MM, PB/SA, and structure-based QSAR analyses. *Amino Acid* 40:493–503
- Tian F, Lv Y, Zhou P, Yang L (2011b) Characterization of PDZ domain–peptide interactions using an integrated protocol of QM/MM, PB/SA, and CFEA analyses. *J Comput Aided Mol Des* 25:947–958
- Veale D, Ashcroft T, Marsh C, Gibson GJ, Harris AL (1987) Epidermal growth factor receptors in non-small cell lung cancer. *Br J Cancer* 55:513–516
- Wang J, Wolf RM, Caldwell JW, Kollman PA, Case DA (2004) Developing and testing of a general amber force field. *J Comput Chem* 25:1157–1174
- Yoshikawa S, Kukimoto-Niino M, Parker L, Handa N, Terada T, Fujimoto T, Terazawa Y, Wakiyama M, Sato M, Sano S, Kobayashi T, Tanaka T, Chen L, Liu ZJ, Wang BC, Shirouzu M, Kawa S, Semba K, Yamamoto T, Yokoyama S (2013) Structural basis for the altered drug sensitivities of non-small cell lung cancer-associated mutants of human epidermal growth factor receptor. *Oncogene* 32:27–38
- Yun CH, Boggon TJ, Li Y, Woo MS, Greulich H, Meyerson M, Eck MJ (2007) Structures of lung cancer-derived EGFR mutants and inhibitor complexes: mechanism of activation and insights into differential inhibitor sensitivity. *Cancer Cell* 11:217–227
- Yun CH, Mengwasser KE, Toms AV, Woo MS, Greulich H, Wong KK, Meyerson M, Eck MJ (2008) The T790M mutation in EGFR kinase causes drug resistance by increasing the affinity for ATP. *Proc Natl Acad Sci USA* 105:2070–2075
- Zhang C, Vasmatazis G, Cornette JL, DeLisi C (1997) Determination of atomic desolvation energies from the structures of crystallized proteins. *J Mol Biol* 267:707–726
- Zhou P, Tian F, Shang Z (2009a) 2D depiction of nonbonding interactions for protein complexes. *J Comput Chem* 30:940–951
- Zhou P, Zou J, Tian F, Shang Z (2009b) Fluorine bonding—how does it work in protein–ligand interactions? *J Chem Inf Model* 49:2344–2355
- Zhou W, Ercan D, Chen L, Yun CH, Li D, Capelletti M, Cortot AB, Chirieac L, Jacob RE, Padera R, Engen JR, Wong KK, Eck MJ, Gray NS, Jänne PA (2009c) Novel mutant-selective EGFR kinase inhibitors against EGFR T790M. *Nature* 462:1070–1074